Table 3 Correlations between clinical findings and hepatic 8-OHdG expression levels in patients with chronic hepatitis C and B

Characteristics	Chronic hepatitis C (n = 77)		Chronic hepatitis B (n = 34)	
	r	P Values	r	P Values
Age (years)	0.140	0.2212	-0.559	0.0013
Body mass index (kg/m^2)	0.265	0.0209	−0.291	0.0944
Laboratory data				
ALT (IU/L)	**0.738**	**<0.0001**	**0.506**	**0.0037**
AST (IU/L)	**0.720**	**<0.0001**	**0.515**	**0.0031**
T-Bilirubin (mg/dL)	0.351	0.0022	0.050	0.7717
T-Cholesterol (mg/dL)	−0.029	0.7994	0.227	0.1924
Hyaluronic acid (ng/mL)	0.226	0.0487	−0.253	0.1453
Platelet count (× 10^4/mm^3)	−0.266	0.0205	0.302	0.0825
Red blood cell count (× 10^4/mm^3)	0.027	0.8147	−0.032	0.8544
Haemoglobin (g/dL)	0.125	0.2768	0.033	0.8516
Serum iron (μg/dL)	0.270	0.0185	−0.078	0.6549
Transferrin saturation (%)	0.318	0.0056	−0.075	0.6664
Serum ferritin (ng/mL)	**0.615**	**<0.0001**	0.064	0.6928
Viral litre				
HCV-RNA (KIU/mL)	−0.024	0.8324	–	
HBV-DNA (LGE/mL)	–		**0.540**	**0.0019**
Liver histology				
Total iron score*	**0.520**	**<0.0001**	−0.126	0.4079
mRNA (/GAPDH)				
TfR2	−0.258	0.0243	−0.167	0.3457
Hepcidin	**0.571**	**<0.0001**	0.070	0.6883

*Histological quantification of iron was assessed by total iron score proposed by Deugnier *et al* (1992).
8-OHdG, 8-hydroxyguanosine; ALT, alanine aminotransferase; AST, aspartate aminotransferase; TfR2, transferrin receptor 2; GAPDH, glyceraldehyde 3-phosphate dehydrogenase.
Bold values indicate that correlations between these two variables are very close ($r > 0.5$).

hepatic hepcidin mRNA expression levels, as a marker for iron overload. A statistically significant positive correlation was also observed between 8-OHdG levels and hepcidin mRNA levels in the liver of patients with CH-C ($r = 0.571$, $P < 0.0001$) (Table 3; Fig. 2e).

Clinical variables that correlate with hepatic oxidative DNA damage in patients with CH-B

The correlation of clinical and histological findings with the degree of hepatic oxidative DNA damage was also evaluated in CH-B patients. Serum transaminase levels were significantly correlated with hepatic 8-OHdG count in CH-B patients (*vs* ALT, $r = 0.506$, $P = 0.0037$; *vs* AST, $r = 0.515$, $P = 0.0031$) (Table 3; Figs 3a,b), although the statistical coefficients of Spearman were smaller compared to those of CH-C. Hepatic 8-OHdG was increased in accordance with the progression of hepatic histological inflammatory grading in CH-B patients, but these differences did not reach statistical significance (Fig. 1d). Unlike cases of HCV infection, hepatic 8-OHdG levels were not related to body and hepatic iron deposition markers (serum ferritin, TIS, hepcidin mRNA levels), but were significantly correlated with individual serum HBV-DNA titres and age of the patients (Table 3; Fig. 3c,d).

DISCUSSION

Especially in the case of HCV infection, underlining mechanisms by which hepatitis viruses cause liver cell injury are largely unknown. Oxidative stress is one of the most probable mediators, because patients with chronic HCV infection show an increase in serum or liver content of oxidative stress markers, such as lipid peroxidation products [20], superoxide dismutase [10], and 8-isoprostane [27]. In this study, using specific and sensitive immunohistochemical staining with anti-8-OHdG antibodies, 8-OHdG positive signals in the liver tissue were detected in all patients examined, indicating that oxidatively generated DNA damage occurs frequently in the liver of patients with chronic HCV and HBV infections. The relatively high 8-OHdG expression levels in our study compared to previous reports [28,29] are most likely related to differences in methodology. Variations in 8-OHdG levels have been

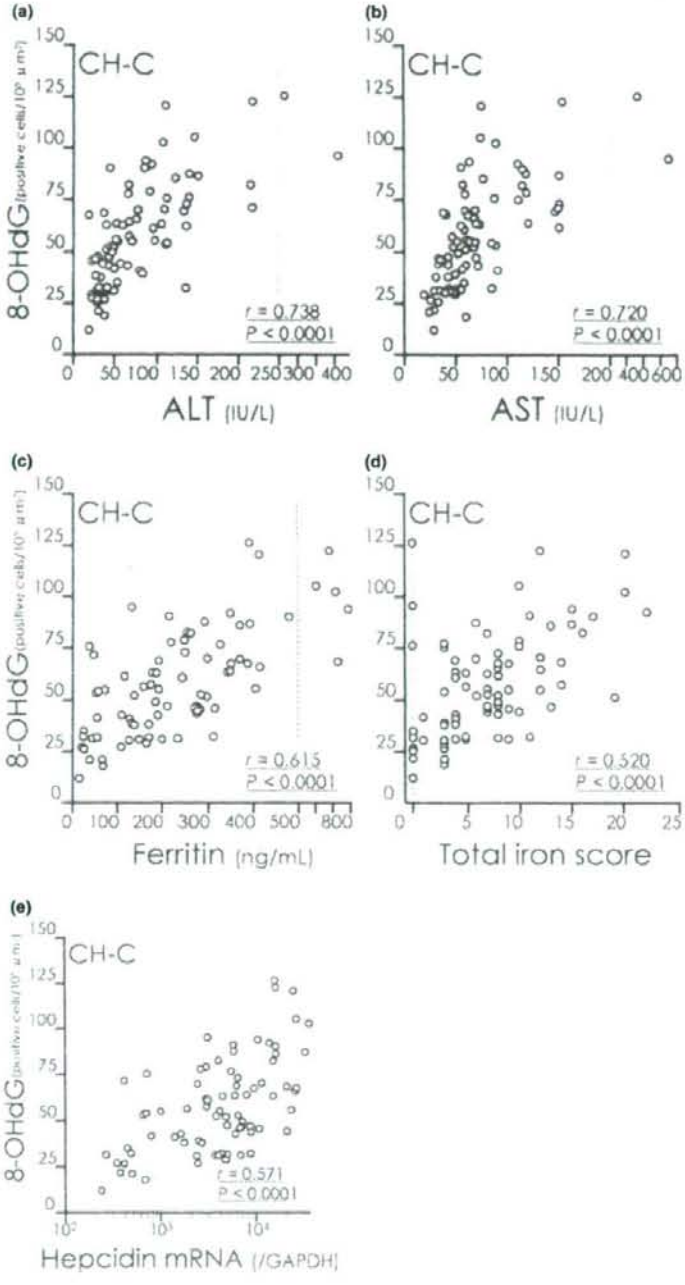

Fig. 2 Correlation between the 8-hydroxydeoxyguanosine (8-OHdG)-positive hepatocytic nuclear count and clinical variables in 77 patients with chronic hepatitis C. (a) 8-OHdG count and serum ALT levels. (b) 8-OHdG count and serum AST levels. (c) 8-OHdG count and serum ferritin levels. (d) 8-OHdG count and total iron score in hepatic tissue. (e) 8-OHdG count and hepcidin messenger RNA levels in hepatic tissue.

reported depending on DNA extraction procedures and detection methods used [30]. Therefore, a comparison of absolute 8-OHdG values between different studies can be done with caution.

The first conclusion of our study is that quantitative hepatocytic 8-OHdG immunoreactivity was significantly correlated with serum transaminase levels, the representative serum marker of hepatic inflammation, both in CH-C

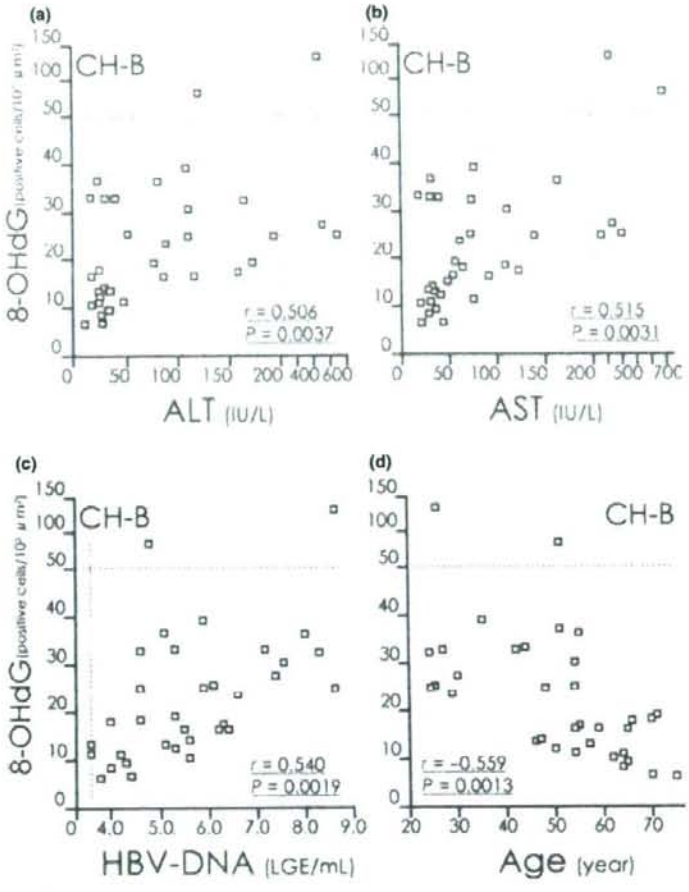

Fig. 3 Correlation between 8-hydroxydeoxyguanosine (8-OHdG)-positive hepatocytic nuclear count and clinical variables in 34 patients with chronic hepatitis B. (a) 8-OHdG count and serum ALT levels. (b) 8-OHdG count and serum AST levels. (c) 8-OHdG count and serum HBV-DNA titers. (d) 8-OHdG count and age of patients.

and CH-B. In the case of HCV, these results are in accordance with previous reports showing that plasma levels of lipid peroxidation products are correlated with aminotransferase levels in CH-C patients [31]. Shimoda *et al.* [28] also established a positive correlation between 8-OHdG concentration of extracted DNA from CH-C liver biopsy specimens and serum ALT activity. A possible link between the degree of hepatic oxidative DNA damage and hepatic inflammation may indicate the direct involvement of hepatic oxidative stress in the pathogenesis and progression of liver cell injury in chronic viral hepatitis. Certainly, it is unclear whether the oxidative stress is the cause or the consequence of liver cell injury from our results, but whichever is correct, hepatic DNA damage could be the cause of hepatocarcinogenesis which is frequently observed during chronic HCV and HBV infection, as 8-OHdG is a promutagenic lesion as it mispairs during DNA replication [4]. Therefore, it is conceivable that the treatment of chronic liver disease to suppress hepatic inflammation may have a preventive benefit for HCC development in chronic hepatitis patients. In fact, clinical studies have suggested that continuous hepatitis with high transaminase activity after curable resection of HCC is an independent risk factor for new development of HCC [32], and that treatment of chronic active hepatitis C with interferon may diminish the incidence of HCC in patients who normalized transaminases, even when viraemia is persistent [33].

Our second major conclusion is that the 8-OHdG-positive hepatocytic count in HCV-infected livers was significantly higher than in HBV-infected ones, suggesting that HCV infection may cause a more advanced oxidative stress in the liver during chronic infection. Because the baseline characteristics including serum aminotransferase levels and histological grading of inflammation were not significantly different between CH-C and CH-B, the difference in the hepatic inflammation status does not seem to be responsible for the abundant hepatic oxidative stress in CH-C patients. Stratifying the patients with histological grade, CH-C

patients in the subgroup with mild to moderate inflammatory activities (grading scores 0/1 and 2) also had significantly higher 8-OHdG levels as compared to CH-B with the same inflammatory activities, indicating that HCV infection itself has a more direct influence on hepatic oxidative stress formation. Most plausible candidate for the source of hepatic oxidative stress formation in CH-C is excessive deposition of iron in the liver, that is frequently implicated in chronic HCV infection [20,21,34], because the serum ferritin levels, that reflect the iron burden in the body of chronic liver disease patients [35], and TIS, the marker of hepatic iron deposition, were significantly higher in CH-C patients than in CH-B. The hepatic 8-OHdG levels were significantly correlated with the ferritin levels and TIS scores, also indicating a strong relationship between the oxidative DNA damage and iron overload status in the liver of patients with CH-C. It is known that free iron promotes generation of oxygen radicals by catalysing the Fenton reaction in which Fe^{2+} reacts with H_2O_2 to generate highly reactive hydroxyl radicals. Therefore, it is plausible that ROS production during chronic HCV infection is the effect of high iron levels in hepatic tissues in CH-C patients, which lead to progressive liver inflammation, and increased risk for developing liver cancer. The mechanisms involved in such a modification of iron metabolism associated with chronic HCV infection remain unclear. We have reported previously that the hepatic TfR2 mRNA expression levels were remarkably increased in CH-C patients [23] and the results were confirmed in this report using another study population. Therefore, hepatic iron overload may be caused by this upregulation of hepatic TfR2 expression in the liver of HCV infected patients. Recently, hepcidin, that is exclusively synthesized in the liver, was identified as a key regulator of body iron balance [25,26]. It has been clearly demonstrated that hepatic hepcidin expression is immediately and strictly regulated in response to hepatic iron levels [25]. In this study, a significant correlation was observed between hepatic 8-OHdG count and hepatic hepcidin expression levels in CH-C patients, also suggesting direct involvement of iron overload in hepatic oxidative stress formation, although the hepcidin expression levels were not significantly different between HCV- and HBV-infected patients. Further studies are necessary to identify the molecular mechanism responsible for iron overload that is frequently seen in CH-C patients.

Hepatic oxidative stress also seems to be concerned with hepatic inflammation in the case of chronic HBV infection, because the serum transaminase levels were significantly correlated with the hepatic 8-OHdG count among the CH-B patients. However, serum ferritin and TIS were not correlated to hepatic 8-OHdG levels in CH-B, therefore the involvement of iron overload for hepatic oxidative stress formation is relatively weak or none in chronic HBV infection. On the other hand, hepatic 8-OHdG levels were positively correlated with serum HBV-DNA titers. Majano *et al.* [36] demonstrated that the HBV genome could directly upregulate nitric oxide synthase 2 (NOS2) gene expression in cultured human hepatocyte-derived cells. The NOS2 gene generated long-term over-production of nitric oxide (NO), resulting in an increase in NO-related DNA damage [37]. Therefore, such a mechanism by which HBV directly induces hepatocarcinogenesis may be involved in the formation of hepatocytic DNA damage in chronic HBV-infected patients. The correlation of hepatic 8-OHdG count with age may be on account of the correlation between age and HBV-DNA titres in these patients ($r = -0.551$, $P = 0.0015$).

In summary, we have demonstrated that oxidative DNA damage widely occurs in the livers of patients with chronic viral hepatitis especially in CH-C, and its relation to serum trasaminase levels indicates that hepatic oxidative stress is one of the mechanisms fuelling necro-inflammatory changes in chronic viral hepatitis. As a matter of fact, it should be noted that 8-OHdG represents an ongoing mutagenic phenomenon even in liver cirrhosis where high transaminase levels are unusual. Thus, hepatic 8-OHdG levels may be the most potent predictive marker for hepatocarcinogenesis during chronic HCV and HBV infection. The strong positive correlations between hepatic oxidative DNA damage and iron overload in CH-C suggest that hepatic iron content is one of the most probable mediators of hepatic oxidative stress in HCV infection, and iron reduction therapy may be beneficial in reducing HCC incidence in CH-C patients.

ACKNOWLEDGEMENTS

This study was supported by a Grant-in-Aid (No. 18590728, 2006-2007) from the Ministry of Education, Science and Culture of Japan.

REFERENCES

1 Valko M, Leibfritz D, Moncol J, Cronin MT, Mazur M, Telser J. Free radicals and antioxidants in normal physiological functions and human disease. *Int J Biochem Cell Biol* 2007; 39: 44–84.
2 Shigenaga M, Gimeno CJ, Ames BN. Urinary 8-hydroxy-2'-deoxyguanosine as a biomarker of *in vivo* oxidative DNA damage. *Proc Natl Acad Sci USA* 1989; 86: 9697–9701.
3 Kasai H. Analysis of a form of oxidative DNA damage 8-hydroxy-2'-deoxyguanosine, as a marker of cellular oxidative stress during carcinogenesis. *Mutat Res* 1997; 387: 147–163.
4 Kuchino Y, Mori F, Kasai H *et al.* Misreading of DNA templates containing 8-hydroxydeoxyguanosine at the modified base and at adjacent residues. *Nature* 1987; 327: 77–79.
5 El-Serag HB. Hepatocellular carcinoma and hepatitis C in the United States. *Hepatology* 2002; 36(Suppl. 1): 74–83.
6 Kiyosawa K, Tanaka E. Characteristics of hepatocellular carcinoma in Japan. *Oncology* 2002; 62(Suppl. 1): 5–7.

7 Stroffolini T, Chiaramonte M, Tiribelli C *et al.* Hepatitis C virus infection, HBsAg carrier state and hepatocellular carcinoma: relative risk and population attributable risk from a case-control study in Italy. *J Hepatol* 1992; 16: 360–363.

8 Ikeda K, Saitoh S, Koida I *et al.* A multivariate analysis of risk factors for hepatocellular carcinogenesis: a prospective observation of 795 patients with viral and alcoholic cirrhosis. *Hepatology* 1993; 18: 47–53.

9 Paradis V, Mathurin P, Kollinger M *et al. In situ* detection of lipid peroxidation of chronic hepatitis C: correlation with pathological features. *J Clin Pathol* 1997; 50: 401–406.

10 Larrea E, Beloqui O, Munoz-Navas MA, Civeira MP, Prieto J. Superoxide dismutase in patients with chronic hepatitis C virus infection. *Free Radic Biol Med* 1998; 24: 1235–1241.

11 Marotta F, Yoshida C, Barreto R, Naito Y, Packer L. Oxidative-inflammatory damage in cirrhosis: effect of vitamin E and a fermented papaya preparation. *J Gastroenterol Hepatol* 2007; 22: 697–703.

12 Barbaro G, Di Lorenzo G, Ribersani M *et al.* Serum and hepatic glutathione concentrations in chronic hepatitis C patients related to hepatitis C virus genotype. *J Hepatol* 1999; 30: 774–782.

13 Mahmood S, Yamada G, Niiyama G *et al.* Effect of vitamin E on serum aminotransferase and thioredoxin levels in patients with viral hepatitis C. *Free Radic Res* 2003; 37: 781–785.

14 Shafritz DA, Kew MC. Integration of hepatitis B virus DNA into the genome of liver cells in chronic liver disease and hepatocellular carcinoma. *New Engl J Med* 1981; 305: 1067–1073.

15 Natoli G, Avantaggiati ML, Chirillo P *et al.* Ras- and Raf-dependent activation of c-jun transcriptional activity by the hepatitis B virus transactivator pX. *Oncogene* 1994; 9: 2837–2843.

16 Huang SN, Chisari FV. Strong, sustained hepatocellular proliferation precedes hepatocarcingenesis in hepatitis B surface antigen transgenic mice. *Hepatology* 1995; 21: 620–626.

17 Desmet VJ, Gerber M, Hoofnagle JH, Manns M, Scheuer PJ. Classification of chronic hepatitis: diagnosis, grading and staging. *Hepatology* 1994; 19: 1513–1520.

18 Deugnier YM, Loreal O, Turlin B *et al.* Liver pathology in genetic hemochromatosis: a review of 135 homozygous cases and their bioclinical correlations. *Gastroenterology* 1992; 102: 2050–2059.

19 Deugnier YM, Turlin B, Powell LW *et al.* Differentiation between heterozygotes and homozygotes in genetic hemochromatosis by means of a histological hepatic iron index: a study of 192 cases. *Hepatology* 1993; 17: 30–34.

20 Piperno A, Vergani A, Malosio I *et al.* Hepatic iron overload in patients with chronic viral hepatitis: role of HFE gene mutations. *Hepatology* 1998; 28: 1105–1109.

21 Silvia IS, Perez RM, Oliveira PV *et al.* Iron overload in patients with chronic hepatitis C virus infection: clinical and histological study. *J Gastroentrol Hepatol* 2005; 20: 243–248.

22 Horiike S, Kawanishi S, Kaito M *et al.* Accumulation of 8-nitroguanine in the liver of patients with chronic hepatitis C. *J Hepatol* 2005; 43: 403–410.

23 Takeo M, Kobayashi Y, Fujita N *et al.* Upregulation of transferrin receptor 2 and ferroportin 1 mRNA in the liver of patients with chronic hepatitis C. *J Gastroenterol Hepatol* 2005; 20: 562–569.

24 Fujita N, Sugimoto R, Takeo M *et al.* Hepcidin expression in the liver: relatively low level in patients with chronic hepatitis C. *Mol Med* 2007; 13: 97–104.

25 Pigeon C, Ilyin G, Courselaud B *et al.* A new mouse liver-specific gene, encoding a protein homologous to human antimicrobial peptide hepcidin, is overexpressed during iron overload. *J Biol Chem* 2001; 276: 7811–7819.

26 Frazer DM, Wilkins SJ, Becker EM *et al.* Hepcidin expression inversely correlates with the expression of duodenal iron transporters and iron absorption in rats. *Gastroenterology* 2002; 123: 835–844.

27 Konishi M, Iwasa M, Araki J *et al.* Increased lipid peroxidation in patients with non-alcoholic fatty liver disease and chronic hepatitis C as measured by the plasma level of 8-isoprostane. *J Gastroenterol Hepatol* 2006; 21: 1821–1825.

28 Shimoda R, Nagashima M, Sakamoto M *et al.* Increased formation of oxidative DNA damage, 8-hydroxydeoxyguanosine, in human livers with chronic hepatitis. *Cancer Res* 1994; 54: 3171–3172.

29 Kato J, Kobune M, Nakamura T *et al.* Normalization of elevated hepatic 8-hydroxy-2'-deoxyguanosine levels in chronic hepatitis C patients by phlebotomy and low iron diet. *Cancer Res* 2001; 61: 8697–8702.

30 Escodd. Comparative analysis of baseline 8-oxo-7, 8-dihydroguanosine in mammalian cell DNA, by different methods in different laboratories: an approach to consensus. *Carcinogenesis* 2002; 23: 2129–2133.

31 Sumida Y, Nakashima T, Yoh T *et al.* Serum thioredoxin levels as an indicator of oxidative stress in patients with hepatitis C virus infection. *J Hepatol* 2000; 33: 616–622.

32 Kubo S, Nishiguchi S, Shuto T *et al.* Effects of continuous hepatitis with persistent hepatitis C viremia on outcome after resection of hepatocellular carcinoma. *Jpn J Cancer Res* 1999; 90: 162–170.

33 Nishikawa M, Nishiguchi S, Kioka K, Tomori A, Inoue M. Interferon reduces somatic mutation of mitochondrial DNA in liver tissues from chronic viral hepatitis patients. *J Viral Hepat* 2005; 12: 494–498.

34 Sebastiani G, Vario A, Ferrari R, Pistis F, Noventa F, Alberti A. Hepatic iron, liver steatosis and viral genotypes in patients with chronic hepatitis C. *J Viral Hepat* 2005; 13: 199–205.

35 Prieto J, Barry M, Sherlock S. Serum ferritin in patients with iron overload and with acute and chronic liver diseases. *Gastroenterology* 1975; 68: 525–533.

36 Majano PL, Monzon CG, Cabrera LC *et al.* Inducible nitric oxide synthase expression in chronic viral hepatitis: evidence for a virus-induced gene upregulation. *J Clin Invest* 1998; 101: 1343–1352.

37 Wink DA, Kasprzak KS, Maragos CM *et al.* DNA deaminating ability and genotoxicity of nitric oxide and its progenitors. *Science* 1991; 254: 1001–1003.

Journal of Thrombosis and Haemostasis, 6: 139–146

ORIGINAL ARTICLE

Protective role of thrombin activatable fibrinolysis inhibitor in obstructive nephropathy-associated tubulointerstitial fibrosis

N. E. BRUNO,* Y. YANO,* Y. TAKEI,† E. C. GABAZZA,*‡ L. QIN,* M. NAGASHIMA,§ J. MORSER,§ C. N. D'ALESSANDRO-GABAZZA,*¶ O. TAGUCHI¶ and Y. SUMIDA*

**Department of Diabetes and Endocrinology, Mie University Graduate School of Medicine, Tsu-city, Mie; †Department of Gastroenterology and Hepatology, Mie University Graduate School of Medicine, Tsu-city, Mie; ‡Department of Immunology and Allergy, Mie University Graduate School of Medicine, Tsu-city, Mie, Japan; §Department of Cardiovascular Research, Berlex Biosciences, Richmond, CA, USA; and ¶Department of Pulmonary and Critical Care Medicine, Mie University Graduate School of Medicine, Tsu-city, Mie, Japan*

To cite this article: Bruno NE, Yano Y, Takei Y, Gabazza EC, Qin L, Nagashima M, Morser J, D'Alessandro-Gabazza CN, Taguchi O, Sumida Y. Protective role of thrombin activatable fibrinolysis inhibitor in obstructive nephropathy-associated tubulointerstitial fibrosis. *J Thromb Haemost* 2008; **6**: 139–46.

Summary. *Background:* Thrombin-activatable fibrinolysis inhibitor (TAFI) has been reported to affect wound healing and fibrotic processes, but its role in renal tubulointerstitial fibrosis remains unknown. *Objective:* To study its potential role, we compared TAFI-deficient and wild-type mice for the degree of renal fibrosis caused by unilateral ureteral obstruction (UUO). *Methods:* The grade of tubulointerstitial fibrosis, the activity of plasmin, MMP-2 and MMP-9 were evaluated on days 4 and 9 after UUO. *Results:* The renal content of hydroxyproline and the activity of plasmin, MMP-2 and MMP-9 were significantly increased in kidneys with UUO from TAFI-deficient mice compared with those from wild-type mice. These differences disappeared when animals with UUO from both groups were treated with the plasmin inhibitor tranexamic acid. The renal concentrations of fibrogenic cytokines were also significantly elevated in kidneys with UUO from TAFI-deficient mice compared with those from wild-type mice. *Conclusion:* The results of this study suggest that increased renal activity of plasmin in TAFI-deficient mice causes increased renal interstitial fibrosis in obstructive nephropathy.

Keywords: coagulation, fibronolysis, metalloproteinases, obstruction, plasmin, renal fibrosis.

Introduction

Renal interstitial fibrosis is a frequent pathological finding in a wide variety of disorders including those associated with obstruction of the renal excretory system [1]. Obstructive nephropathy is characterized by increased infiltration of monocytes/macrophages, increased activation of myofibroblasts, tubular atrophy and augmented synthesis and accumulation of extracellular matrix (ECM) proteins in the renal interstitium [1,2]. A recent study, showing that mice deficient in plasminogen had decreased obstructive nephropathy-associated renal interstitial fibrosis compared with their wild-type counterparts, suggests that plasmin is profibrotic in this model [3].

In theory, plasmin can be profibrogenic by its ability to stimulate the recruitment of leukocytes [4], to activate the latent form of transforming growth factor-β (TGF-β) and to increase the release of TGF-β bound to matrix components [5]. Plasmin can also stimulate fibrosis by activating MMPs, which causes tubular basement membrane disruption, or by promoting tubular epithelial-to-mesenchymal transition [6]. The regulator of this profibrotic action of plasmin remains unknown. The profibrogenic action of plasmin was reported to be independent of the effects of tissue plasminogen activator and plasminogen activator inhibitor-1 (PAI-1) [7–9]. Another potential regulator of plasmin generation is thrombin-activatable fibrinolysis inhibitor (TAFI). TAFI is an acute reactant protein (55 kD) produced in the liver and secreted in zymogen form. TAFI is activated by thrombin, plasmin and the thrombin–thrombomodulin complex. The active form of TAFI inhibits fibrinolysis by blocking directly the action of plasmin or cleaving the carboxy-terminal lysine residues from partially degraded fibrin [10,11]. In this study, we hypothesize that TAFI-mediated decreased plasmin generation ameliorates unilateral ureteric obstruction (UUO)-induced renal interstitial fibrosis.

Materials and methods

Animals

TAFI knockout mice, originally generated and characterized by Nagashima *et al.* [12], were backcrossed with C57BL/6 mice

Correspondence: Esteban C. Gabazza, Department of Immunology and Allergy, Mie University Graduate School of Medicine, Edobashi 2-174, Tsu-city, Mie 514-8507, Japan.
Tel.: +81 59 231 3180; fax: +81 59 231 5223; e-mail: gabazza@clin.medic.mie-u.ac.jp

Received 12 April 2007, accepted 21 October 2007

for more than ten generations before being used in the experiments. Mice were housed on a constant 12-h light/12-h dark cycle in a temperature- and humidity-controlled room, with free access to standard chow and water. Male TAFI knockout mice and wild-type littermates between 8 and 10 weeks of age were used in the experiments.

Animal model of UUO

Three groups of male, weight-matched, TAFI knockout and wild-type mice were used in the experiments: sham-operated mice with normal urinary tract (SHAM), wild-type mice with left ureteral obstruction (WT/UUO) and TAFI-deficient mice with left ureteral obstruction (KO/UUO). The contralateral kidneys in both genetic groups (WT/CONT) and (KO/CONT) served as intraindividual controls. UUO was performed in sterile conditions under general anesthesia performed with Nembutal® (Dainippon Pharmaceutical Co. Ltd, Osaka, Japan). The left ureter was exposed through a mid-abdominal incision and double-ligated at the uretero-pelvic junction. Sham-operated animals underwent identical surgical procedures but without ureteral ligation. Plasma and both control kidneys of SHAM mice and the obstructed kidney and the intact right contralateral kidney of UUO mice were collected on days 4 (n = 6 in each group) and 9 (n = 8 in each group) after operation.

To investigate the role of plasmin activity, WT and TAFI KO mice (n = 6 in each group) were treated with tranexamic acid (Sigma-Aldrich, St Louis, MO, USA) during the UUO model. Tranexamic acid was administered by daily subcutaneous injection (1.8 mg per day) plus oral ingestion by adding it to drinking water at a concentration of 20 mg mL^{-1} following previously described methods [13]. All mice were killed by exsanguination under general anesthesia. The Mie University's Committee on animal investigation approved the experimental protocol, and the experiments were performed according to the guidelines for animal experiments of the National Institute of Health.

Preparation of renal tissues

After killing the animals under anesthesia, the left kidney was harvested, washed in ice-cold phosphate-buffered saline (PBS) and the renal capsule was removed. The right kidney was treated in the same way and used as intraindividual control. Both the left and right kidneys were then cut and separated into two pieces by sagittal section; one half was used for preparation of paraffin sections and the other half was homogenized for 2 min in a protease inhibitor cocktail without ethylenediamine tetraacetic acid (Nacalai Tesque, Kyoto, Japan) using a Polytron homogenizer (Kinematica GmbH, Littau-Lucerne, Switzerland). The homogenates were then centrifuged (15 000 × g) at 4 °C and the supernatants stored in small aliquots at −80 °C until use. Protein concentration in the homogenates was measured using the BCA™ protein assay kit purchased from Pierce (Rockford, IL, USA).

Measurement of interstitial expansion

Renal interstitial space, defined as the area not occupied by glomeruli, tubules or vessels, was estimated using image processing software (WinRoof Mitani Corp., Fukui, Japan), as previously reported [14]. Briefly, five randomly selected cortical fields, from periodic acid shif (PAS) stained paraffin sections, were photographed under high magnification (400×) using a spot digital camera (Olympus DP70 Digital Camera, Tokyo, Japan). Next, the areas occupied by glomeruli, tubules and vessels were outlined and cut out from the image. The PAS (+) interstitial space is reported as the percentage of the total image area (n = 6).

Measurement of hydroxyproline

Total renal hydroxyproline content was measured by a colorimetric method as previously described [15].

Western blotting

Protein was extracted from renal tissue from each group of mice using lysis buffer containing a protease inhibitor cocktail without ethylenediamine tetraacetic acid (Nacalai Tesque, Kyoto, Japan). Protein concentrations were determined by using a BCA Protein Assay Kit (Pierce). Fibrin(ogen) in the samples was immunoprecipitated using rabbit antifibrin(ogen) antibody (Dako A/S, Glostrup, Denmark) and protein G microbeads (Miltenyi Biotec, Bergidch Gladbach, Germany). Then the proteins were fractionated on sodium dodecylsulfate (SDS)-polyacrylamide gels and transferred to a polyvinyldifluoride membrane. The membrane was then probed with antifibrin(ogen) and horseradish peroxidase-labeled goat anti-rabbit antibody. The membrane was washed and quantitated using an enhanced chemiluminescence detection system (ECL; Amersham, Buckinghamshire, UK).

Biochemical analysis

The levels of monocyte chemoattractant protein-1 (MCP-1), TGF-β1, interleukin(IL)-6 and IL-1β were measured using enzyme immunoassay kits from BD Biosciences Pharmingen (San Diego, CA, USA), and fibrin(ogen) was measured using (Dako A/S, Glostrup, Denmark) antibodies. The levels of tissue-type plasminogen activator (t-PA) and urokinase-type plasminogen activator (u-PA) were measured spectrophotometrically using the synthetic chromogenic substrates S-2288 and S-2444 (Chromogenix, Molndal, Sweden). The level of mouse PAI-1 was measured by enzyme immunoassay using a primary monoclonal antibody specific for mouse PAI-1 and biotin-labeled anti-PAI-1 antibody. Plasmin activity in renal tissue and plasma was determined using a plasmin-specific chomogenic substrate S-2251 (Chromogenix, Molndal, Sweden). In brief, 100 μL of renal homogenate or plasma from each mouse was placed in wells of a 96-well plate and then 100 μL (1/10) of the chromogenic substrate was added to the

duplicated samples. Release of *p*-nitroaniline was measured at 405 nm after 10, 30 and 60 min of incubation. Standard curves were generated using human plasmin (Haematologic Thechnologies Inc., Essex Junction, VT, USA).

Zymographic analysis

The activity of metalloproteinases was measured by gelatin zymography using a commercial kit from Invitrogen Life Technology (Carlsbad, CA, USA). 15 μg of sample were loaded in 10% zymogram gelatin gels under non-denaturating conditions. Human MMP-2 and MMP-9 (Chemicon International, Temecula, CA, USA) were used as positive controls. Following electrophoresis, the gel was then incubated in developing solution and stained using the Novex Colloidal Blue Staining Kit from Invitrogen. Photographs were analyzed using WinRoof image analysis software. Activity of plasmin in plasma was also analyzed by zymographic analysis. In brief, 12% SDS-polyacrylamide gels were prepared containing 0.012% fibrinogen and thrombin (10 NHIU ml^{-1}). 5 μL of plasma from each group of mice were dissolved in electrophoresis sample buffer without mercaptoethanol, applied to the gel and separated electrophoretically. The gels were washed in 2.5% Triton X-100, incubated overnight at 37 °C, and then stained with Coomassie blue.

Reverse transcriptase-polymerase chain reaction for gene expression

For evaluation of TAFI gene expression, total RNA was extracted from renal and liver tissues by the guanidine isothiocyanate procedure, using TRIzol reagent (GIBCO Life Technologies, Grand Island, NY, USA). 2 μg of total RNA were reverse transcribed with oligo(dT) primers and then the cDNA was amplified by polymerase chain reaction (PCR), using a SuperScript preamplification system kit (GIBCO Life Technologies) according to the manufacturer's instructions and a thermal cycle program (ASTEC, Fukuoka, Japan). The sequences of mouse TAFI primers used in the experiments were as follows: sense primer, CTGAACAGCATCCTGACA, and antisense primer, GCAGGTGAAATCCATTCTCTGGC. The sequences of glyceraldehyde-3-phosphate dehydrogenase (GAPDH) primers were as follows: sense primer, TGCTGAGTATGTCGTGGAGTCTA, and antisense primer, AGTGGGAGTTGCTGTTGAAGTCG.

Statistical analysis

Data are expressed as the mean ± standard error of the mean. Statistical differences between groups were evaluated by one-way analysis of variance with Newman–Kleus test as *post hoc* analysis or by Student's *t*-test when two groups were compared. A value of $P < 0.05$ was considered as statistically significant. All statistical analyses were performed using the Graph pad software package (Graph pad, San Diego, CA, USA).

Results

Pathological findings

The kidneys with UUO from both wild-type and TAFI KO mice developed progressive renal cortical thinning and tubulointerstitial fibrosis on days 4 and 9 compared to contralateral kidneys without ureteral obstruction. These pathological changes were significantly more prominent in TAFI-deficient mice than in wild-type mice (data not shown). Renal interstitial (peritubular) space was measured as a marker of tubulointerstial fibrosis (Fig. 1A); there was a significant interstitial expansion in both WT/UUO and KO/UUO groups compared to WT/CONT and KO/CONT groups but the interstitial expansion in KO/UUO was significantly enhanced in KO/UUO mice compared to WT/UUO mice (Fig. 1B). The hydroxyproline content, another marker of tissue fibrosis, was significantly higher in the kidneys from KO/UUO mice than in those from WT/UUO mice (Fig. 1C). The disease progressed with time, as the hydroxyproline content in samples taken after 9 days (Fig. 1C) was higher than that taken after 4 days (Fig. 1D). No significant difference was observed in the hydroxyproline content between the WT/CONT and KO/CONT groups (Fig. 1C,D).

Activity of plasmin, t-PA and u-PA

The activity of plasmin, t-PA, u-PA was measured in mice with UUO after 9 days. The renal activity of plasmin was not significantly different between SHAM and WT/UUO mice; however, renal plasmin activity was significantly higher in KO/UUO mice than in SHAM or WT/UUO mice (Fig. 1E). Treatment of wild-type and TAFI-deficient mice with tranexamic acid caused equalization of renal plasmin in the kidneys from WT/UUO and KO/UUO mice (Fig. 1E). The activity of plasmin in plasma as measured by amidolytic assay (Fig. 1F) and zymography (Fig. 1G) was not significantly diferent among the groups. The renal activity of t-PA was significantly enhanced in both WT/UUO and KO/UUO groups compared to the SHAM group, but it was significantly higher in KO/UUO than in WT/UUO mice (Fig. 1H). Urokinase activity was also significantly enhanced in KO/UUO and WT/UUO groups compared to the SHAM group but no significant diferense was found between KO/UUO and WT/UUO groups (Fig. 1I).

Renal level of PAI-1 and activity of MMPs

PAI-1 expression was significantly enhanced in the obstructed kidneys of both the KO/UUO and WT/UUO groups compared to the control groups, but it was not significantly different between the KO/UUO and WT/UUO groups (Fig. 2A). The activity of MMP-2 was undetectable in the WT/CONT and WT/UUO groups, but it was clearly present in the KO/UUO group (Fig. 2B,C). The activity of MMP-9 was undetectable in the WT/CONT and KO/CONT groups; it was detected in the WT/UUO group, but its activity was

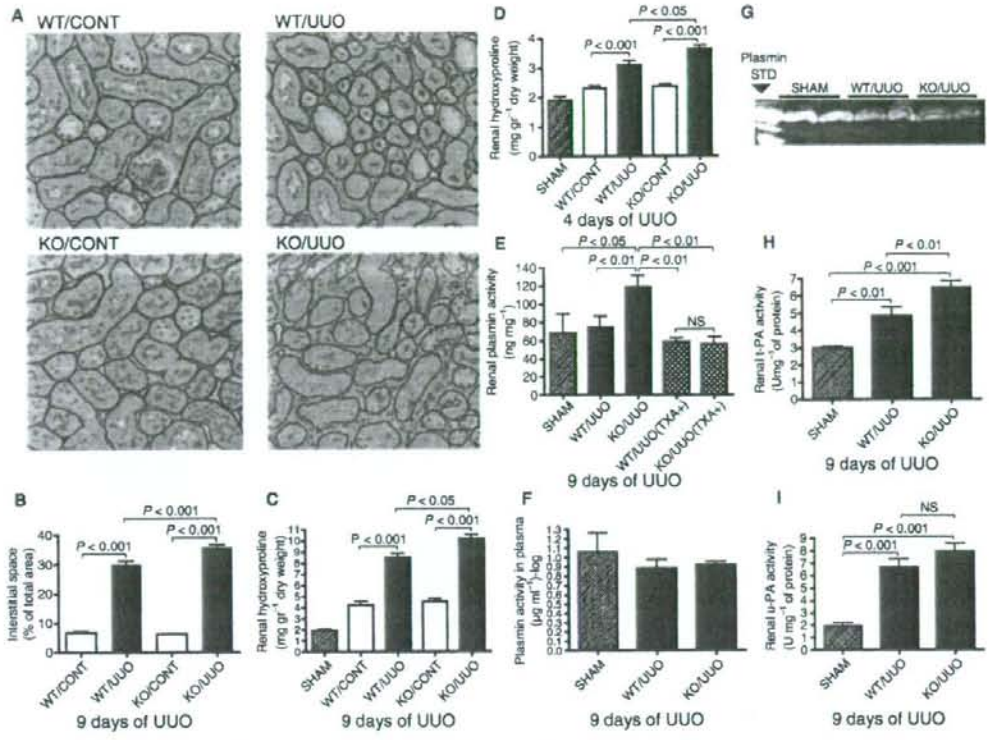

Fig. 1. Renal fibrosis and activity of fibrinolytic factors. The tubulointerstitial space after 9 days of unilateral ureteral obstruction (UUO) was quantified using WinRoof image analizer software (A, B). Renal hydroxyproline content was determined by colorimetric assay after nine (C) and four (D) days of UUO. The activity of plasmin was assessed in renal tissue homogenates (E) and in plasma (F) by amidolytic assay using a specific substrate for plasmin; the activity of plasmin was also measured in plasma by fibrin zymography (G). The activity of tissue-type plasminogen activator (H) and urokinase plasminogen activator (I) in renal tissue homogenates were measured by amidolytic assays. Data are expressed as the mean ± SEM (n = 5–8). Statistical significance between the groups was analyzed by ANOVA and *post hoc* using the Newman–Kleus test.

significantly higher in KO/UUO mice than in the WT/UUO group (Fig. 1B,D).

Fibrin(nogen) accumulation

Ureteral obstruction increased the fibrin(nogen) deposition in both WT/UUO and KO/UUO mice compared to their respective contralateral control kidneys (Fig. 2E). Quantitative analysis performed by EIA showed significantly enhanced concentration of fibrin(ogen) in the WT/UUO (1811 ± 156 μg mg^{-1} of protein, n = 5) and KO/UUO (1518 ± 167 μg mg^{-1} of protein, n = 5) groups compared to the WT/CONT (580 ± 94 μg mg^{-1} of protein, n = 5) and KO/CONT (386 ± 77 μg mg^{-1} of protein, n = 5) groups, respectively. However, there was no statistically significant difference in the renal concentration of fibrin(ogen) between WT/UUO and KO/UUO mice.

Effect of tranexamic acid treatment

Tranexamic acid is a well-known inhibitor of plasminogen conversion to plasmin. Treatment of wild-type and TAFI-deficient mice with tranexamic acid caused equalization of hydroxyproline content in the kidneys from WT/UUO and KO/UUO mice (Fig. 2G,H). Moreover, there was a decrease in gelatinolytic activity shown by reductions in the activity of MMP-2 and MMP-9 when the KO/UUO [KO/UUO(TXA–)] mice were treated with tranexamic acid [KO/UUO(TXA+)] (Fig. 3A,B).

Concentration of cytokines and chemokines

The concentration of TGF-β1, IL-1β (Fig. 3D) and MCP-1 (Fig. 3E) in renal tissue homogenates and the plasma level of IL-1β (Fig. 3F) were significantly elevated in KO/UUO mice compared to WT/UUO mice 9 days after UUO. The renal concentration of TGF-β1 was significantly inhibited by tranexamic acid treatment in both WT/UUO and KO/UUO groups; there was no significant difference between the WT/UUO and KO/UUO groups after treatment with tranexamic acid (Fig. 3D). In addition, the plasma concentration of IL-6 (Fig. 3G) was also significantly increased in KO/UUO mice 4 days after UUO compared to SHAM and WT/UUO mice.

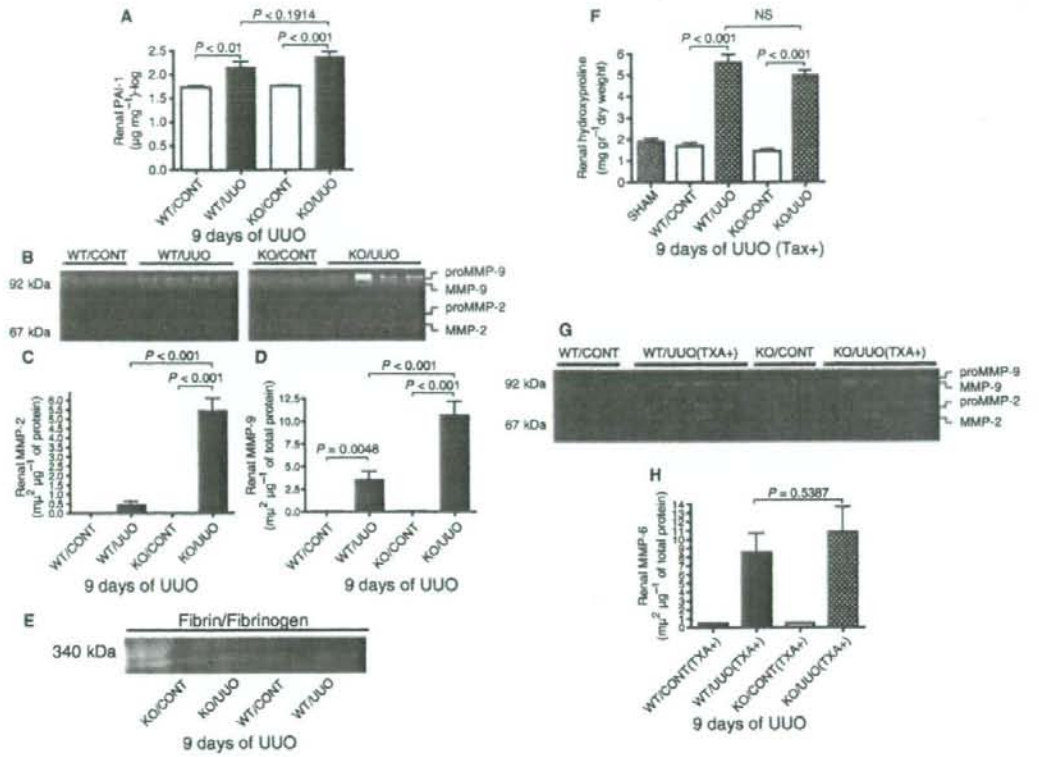

Fig. 2. Renal concentration of plasminogen activator inhibitor-1 (PAI-1), fibrin(ogen) and effect of tranexamic acid. (A) PAI-1 in renal tissue homogenates was measured using a specific EIA (n = 5). (B–D) The gelatinolytic activities of MMP-2 and MMP-9 were measured by zymography (n = 5–8). (E) Fibrin(ogen) was measured by Western blotting. The concentrations of hydroxyproline (F) and MMP-9 (G, H) in renal tissue homogenates from mice treated with tranexamic acid were determined by amidolytic assay, colorimetric assay and gelatin zymography, respectively (n = 5–8). Data are expressed as the mean ± SEM. Statistical significance between the groups was analyzed by ANOVA and *post hoc* using the Newman–Kleus test.

Expression of TAFI in renal tissues

Expression of TAFI was detected in renal tissue and the liver (positive control) as measured by reverse transcription polymerase chain reaction (RT-PCR; Fig. 3H). Comparison of TAFI expresion between samples taken from mice with and without UUO after 9 days (Fig. 3I) showed no difference.

Discussion

This study demonstrates that mice deficient in TAFI have increased activity of plasmin and metalloproteinase and enhanced collagen deposition in the renal interstitium compared to wild-type mice.

Components of the fibrinolysis system include t-PA, urokinase, u-PA receptor, plaminogen, and inhibitors of plasmin generation such as PAI-1 and TAFI [16]. Differential roles have been ascribed to these proteins in the pathogenesis of renal fibrosis, particularly in the process of fibrogenesis following UUO. Plasmin was reported to enhance renal interstitial fibrosis in the UUO model by increasing epithelial–mesenchymal transition and by promoting the activation of TGF-β1 and MMP-2 [3,6]. Independently of plasmin generation, urokinase, u-PA receptor, t-PA and PAI-1 were reported to affect the development of tubulointerstitial fibrosis. t-PA enhances renal fibrosis by enhancing MMP-9 activation, and PAI-1 by increasing inflammatory cell infiltration, matrix turnover and the inhibition of urokinase activity [7–9]. The cellular receptors of urokinase have been reported to protect against renal fibrosis by modulating the clearance of angiogenic and profibrotic molecules during renal injury [17,18]; however, endogenous urokinase was found to exert no antifibrotic effect in the UUO model [19].

In this study, we evaluated the role of TAFI in renal tubulointerstitial fibrosis using the model of UUO. We found that the renal content of hydroxyproline, an indicator of tissue fibrosis, was significantly increased in TAFI-deficient mice on days 4 and 9 after ureteral obstruction compared with their wild-type counterparts. This suggests that TAFI protects against UUO-related renal interstitial fibrosis.

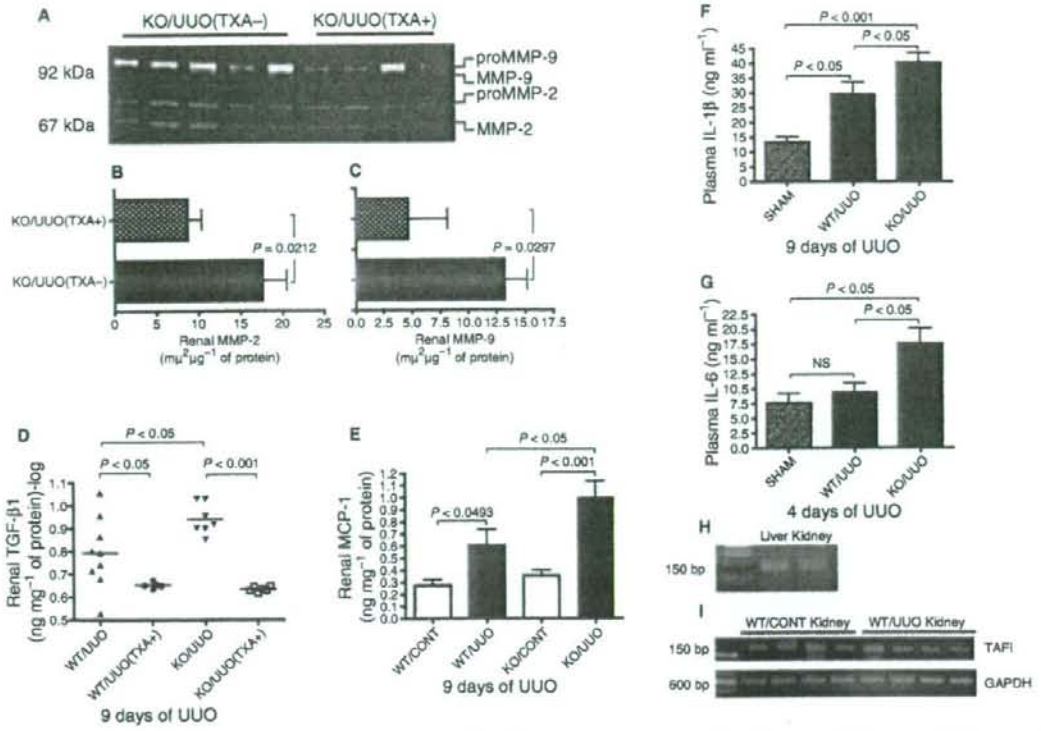

Fig. 3. Concentration of cytokines, effect of tranexamic acid on MMP activity and expression of thrombin-activatable fibrinolysis inhibitor (TAFI) in the kidneys. (A) The activities of MMP-2 and MMP-9 in TAFI knockout (KO) mice treated with tranexamic acid (KO/UUO TXA +) or untreated controls (KO/UUO TXA–) as measured by zymography (n = 6). (B), (C) The results of the densitometric analyses. Data are expressed as the mean ± SEM. Statistical significance between groups was analyzed by the Student t-test. (D) Transforming growth factor-β1 activity in tissue homogenets, (E) the renal concentration of MCP-1, and the plasma levels of (F) IL-1β and (G) IL-6 were measured using specific EIA kits (n = 5–9). Data are expressed as the mean ± SEM. Statistical significance between the groups was analyzed by ANOVA and *post hoc* using the Newman–Kleus test. (H) The RNA expression of TAFI in renal and liver tissues as evaluated by reverse transcription polymerase chain reaction. (I) The renal RNA expression of TAFI in the non-obstructed (CONT/WT) and obstructed (UUO/WT) kidneys of mice after 9 days of obstruction (n = 4).

To clarify the mechanism by which TAFI protects against renal fibrosis, we measured the renal activity of plasmin and metalloproteinase, and found that the activity of these proteases was significantly increased in kidneys with UUO from TAFI-deficient mice compared with that from wild-type mice. This observation suggests that there is a link between enhanced plasmin activity and interstitial fibrosis in the model of UUO. Inhibition of plasmin activity in our model (by treating the mice with tranexamic acid) equalized the renal deposition of hydroxyproline in both TAFI-deficient and wild-type mice, confirming that renal interstitial fibrosis in UUO with TAFI deficiency was caused by increased plasmin activity. Interestingly, we found that plasmin activity in plasma is no different between TAFI-deficient and wild-type mice with ureteral obstruction, suggesting that plasmin is locally generated in the kidneys. Zhang *et al.* [6] reported an increased activity of plasmin in wild-type mice with ureteral obstruction compared to SHAM mice, whereas we found only a slight increased plasmin activity in wild-type mice with the renal obstructive disease compared to SHAM mice. This discrepancy may be explained by the different assays used in both studies. The profibrotic effect of plasmin may be explained by its ability to stimulate the infiltration of inflammatory cells at sites of tissue injury or to promote the activation of TGF-β1 or its release from matrix components [3–5]. Plasmin may also contribute to renal fibrosis by activating pro-MMPs, particularly MMP2 and MMP-9, which are known to promote fibrosis by inducing epithelial–mesenchymal transformation [6]. In line with this, we found increased activity of MMP-2 and MMP-9 in TAFI-deficient mice with UUO compared with their wild-type counterparts.

The hallmark of renal fibrosis is the increased and abnormal deposition of collagen in the tubulointerstitial spaces of the kidneys. Excessive deposition of collagen in the kidneys may result from disruption of the balance between processes of synthesis and degradation of extracellular matrix proteins [20]. This balance is regulated by a complex network of cytokines (IL-1β, IL-6), chemokines (MCP-1) and growth factors (TGF-β1). IL-1β, MCP-1, IL-6, and TGF-β1 promote tissue fibrosis by stimulating the secretion and deposition of

collagens and TGF-β1 after tissue injury or matrix destruction [21,22]. TGF-β1 may also promote collagen deposition by stimulating the secretion of tissue-type metalloproteinase inhibitors or by accelerating the epithelial–mesenchymal transition [21]. In the present study, we found significantly increased concentrations of TGF-β1 and MCP-1 in the kidneys with ureteral obstruction from TAFI-deficient and wild-type mice compared to those from the contralateral unobstructed kidneys. In addition, the plasma concentrations of IL-1β and IL-6 were also significantly elevated in mice with UUO compared with the SHAM group. These observations emphasize the critical role of these inflammatory mediators in the pathogenesis of UUO-related fibrosis. However, the concentrations of TGF-β1 and MCP-1 in the kidneys and the plasma concentrations of IL-1 and IL-6 were significantly elevated in TAFI-deficient mice with UUO compared to their wild-type counterparts, suggesting the protective role of TAFI in UUO. It is worth noting that UUO-related renal fibrosis may also occur independently from the fibrogenic action of TGF-β1 [23].

We have previously reported that deficiency in TAFI is associated with decreased deposition of fibrin and collagen in a mouse model of lung fibrosis, and that this effect is abrogated by depleting the circulating level of fibrinogen, which suggests that decreased generation of plasmin by TAFI favors fibrogenesis in the lung [15]. Enhancement of renal fibrosis by excessive deposition of fibrin has been also reported in models of chronic glomerulonephritis and glomerulosclerosis [24–28]. However, the role of fibrin deposition in obstructive nephropathy-associated tubulointerstitial fibrosis is unknown. In this study, we found no difference in renal fibrin deposition between TAFI-deficient and wild-type mice with ureteral obstruction, indicating that renal fibrosis is independent of fibrin in UUO. This observation suggests that the influence of plasmin on fibrogenesis is organ-specific.

In summary, the results of this study show that increased renal activity of plasmin in TAFI-deficient mice is associated with increased tubulointerstitial fibrosis in obstructive nephropathy. This observation suggests that TAFI may be a potential molecular target for the therapy of obstructive nephropathy.

Addendum

N. Bruno prepared the mouse model of UUO and wrote the initial draft of the manuscript. Y. Yano provided several experimental materials and measured the levels of cytokines. Y. Takei analyzed and interpretated the data. E. C. Gabazza revised the manuscript and performed Western blotting and PCR. L. Qin participated in the preparation of UUO mouse model. M. Nagashima and J. Morser prepared the TAFI knockout mice and made important intellectual contributions. C. N. D'Alessandro-Gabazza prepared the histological samples and performed immunohistochemistry. O. Taguchi was involved in the interpretation of data and in the revision of the manuscript. Y. Sumida coordinated the whole study.

Acknowledgements

This investigation was supported by Grants-in-Aid (nos. 18590846 and 17590788) from the Ministry of Education, Culture, Sports, Science and Technology of Japan, and by Grants-in-Aids from the Mie Medical Research Foundation (2006), the Okasan-Kato Research Foundation (2007) and the Suzuken Memorial Foundation (2005).

Disclosure of Conflict of Interests

The authors state that they have no conflict of interest.

References

1 Eddy AA. Molecular basis of renal fibrosis. *Pediatr Nephrol* 2000; **15**: 290–301.
2 Bascands JL, Schanstra JP. Obstructive nephropathy: insights from genetically engineered animals. *Kidney Int* 2005; **68**: 925–37.
3 Edgtton KL, Gow RM, Kelly DJ, Carmeliet P, Kitching AR. Plasmin is not protective in experimental renal interstitial fibrosis. *Kidney Int* 2004; **66**: 455–6.
4 Syrovets T, Tippler B, Rieks M, Simmet T. Plasmin is a potent and specific chemoattractant for human peripheral monocytes acting via a cyclic guanosine monophosphate-dependent pathway. *Blood* 1997; **89**: 4574–83.
5 Pedrozo HA, Schwarstz Z, Robinson M, Gomes R, Dean DD, Bonewald LF, Boyan BD. Potential mechanisms for plasmin-mediated released and activation of latent transforming growth factor-beta1 from the extracellular matrix of growth plate chondrocytes. *Endocrinology* 1999; **140**: 5806–16.
6 Zhang G, Kernan KA, Collins SJ, Cai X, Lopez-Guiza JM, Degen JL, Shvil Y, Eddy AA. Plasmin(ogen) promotes renal interstitial fibrosis by promoting epithelial-to-mesenchimal transition: role of plasmin-activated signals. *J Am Soc Nephrol* 2007; **18**: 846–59.
7 Oda T, Jung YO, Kim HS, Cai X, López-Guisa JM, Ikeda Y, Eddy AA. PAI-1 deficiency attenuates the fibrogenic response to ureteral obstruction. *Kidney Int* 2001; **60**: 587–96.
8 Matsuo S, Lopez-Guisa JM, Cai X, Oda T, Jung YO, Kim HS, Cai X, Lopez-Guisa JM, Ikeda Y, Eddy AA. Multifunctionality of PAI-1 fibrogenesis: evidence from obstructive nephropathy in PAI-1-over-expressing mice. *Kidney Int* 2005; **68**: 910.
9 Yang J, Shultz RW, Mars WM, Wegner RE, Li Y, Dai C, Nejak K, Liu Y. Disruption of tissue-type plasminogen activator gene in mice reduces renal interstitial fibrosis in obstructive nephropathy. *J Clin Invest* 2002; **110**: 1525–38.
10 Bajzar L. Thrombin activatable fibrinolysis inhibitor and an anti-fibrinolytic pathway. *Arterioscler Thromb Vasc Biol* 2000; **20**: 2511–8.
11 Sato T, Miwa T, Akatsu H, Matsukawa N, Obata K, Okada N, Campbell W, Okada H. Pro-carboxipeptidase R is an acute phase protein in mouse, whereas carboxypeptidase N is not. *J Immunol* 2000; **165**: 1053–8.
12 Nagashima M, Yin ZF, Zhao L, White K, Zhu Y, Lasky N, Halks-Miller M, Broze GJ Jr, Fay WP, Morser J. Thrombin-activatable fibrinolysis inhibitor (TAFI) deficiency is compatible with murine life. *J Clin Invest* 2002; **2109**: 101–10.
13 Hertig A, Berrou J, Allory Y, Breton L, Commo F, Costa De Beauregard MA, Carmeliet P, Rondeau E. Type 1 plasminogen activator inhibitor deficiency aggravates the course of experimental glomerulonephritis through overactivation of transforming growth factor beta. *FASEB J* 2003; **17**: 1904–6.
14 Welch TR, Frenzke M, Witte D, Davis AE. C5a is important in the tubulointerstitial component of experimental immune complex glomerulonephritis. *Clin Exp Immunol* 2002; **130**: 1–3.

15 Fujimoto H, Gabazza EC, Taguchi O, Nakahara H, Bruno NE, D'Alessandro-Gabazza CN, Kasper M, Yano Y, Nagashima M, Morser J, Broze GJ, Suzuki K, Adachi Y. Thrombin-activatable fibrinolysis inhibitor deficiency attenuates bleomycin-induced lung fibrosis. *Am J Pathol* 2006; **168**: 1086–96.
16 Mosesson MW. Fibrinogen and fibrin structure and functions. *J Thromb Haemost* 2005; **3**: 1894–904.
17 Zhang G, Kim H, Cai X, Lopez-Guisa JM, Alpers CE, Liu Y, Carmeliet P, Eddy AA. Urokinase receptor deficiency accelerates renal fibrosis in obstructive nephropathy. *J Am Soc Nephrol* 2003; **14**: 1254–71.
18 Zhang G, Kim H, Cai X, Lopez-Guisa JM, Carmeliet P, Eddy AA. Urokinase receptor modulates cellular and angiogenic responses in obstructive nephropathy. *J Am Soc Nephrol* 2003; **14**: 1234–53.
19 Yamaguchi I, Lopez-Guisa JM, Cai X, Collins SJ, Okamura DM, Eddy AA. Endogenous urokinase lacks anti-fibrotic activity during progressive renal injury. *Am J Physiol Renal Physiol* 2007; **293**: F12–9.
20 Schnaper HW. Balance between matrix synthesis and degradation: a determinant of glomerulosclerosis. *Pediatr Nephrol* 1995; **9**: 104–11.
21 Liu Y. Renal fibrosis: new insights into the pathogenesis and therapeutics. *Kidney Int* 2006; **69**: 213–7.
22 Wynn TA. Common and unique mechanisms regulate fibrosis in various fibroproliferative diseases. *J Clin Invest* 2007; **117**: 524–9.
23 Ma LJ, Yang H, Gaspert A, Carlesso G, Barty MM, Davidson JM, Sheppard D, Fogo AB. Transforming growth factor-beta-dependent and -independent pathways of induction of tubulointerstitial fibrosis in beta6(−/−) mice. *Am J Pathol* 2003; **163**: 1261–73.
24 Herting A, Rondeau E. Role of the coagulation/fibrinolysis system in fibrin-associated glomerular injury. *J Am Soc Nephrol* 2004; **15**: 844–53.
25 Lee HB, Ha H. Plasminogen activator inhibitor-1 and diabetic nephropathy. *Nephrology (Carlton)* 2005; **10**: S11–3.
26 Kamar M, Nobakhthaghighi N, Shamshiraz AA, Estacio RO, McFann KK, Schrier RW. Impared fibrinolytic activity in type II diabetes. *Kidney Int* 2006; **69**: 1899–903.
27 Fogo AB. Mechanism of nephrosclerosis and hypertension-beyon hemodynamics. *J Nephrol* 2001; **14**: S63–9.
28 Opatrny K Jr, Zemanova P, Optrna S, Vit L. Fibrinolysis in chronic renal failure, dialysis and renal transplantation. *Ann Transplant* 2002; **7**: 34–43.

Alimentary Pharmacology & Therapeutics

Predictive factors for distant recurrence of HCV-related hepatocellular carcinoma after radiofrequency ablation combined with chemoembolization

H. FUKE*, K. SUGIMOTO*, K. SHIRAKI*, J. TANAKA*, T. BEPPU*, K. YONEDA*, N. YAMAMOTO*, K. ITO*, H. TAKAKI†, A. NAKATSUKA†, K. YAMAKADO†, K. TAKEDA† & Y. TAKEI*

*Department of Gastroenterology and †Department of Radiology, Mie University School of Medicine, Tsu, Mie, Japan

Correspondence to:
Dr K. Shiraki, Department of Gastroenterology, Mie University School of Medicine, 2-174, Edobashi, Tsu, Mie 514-8507, Japan.
E-mail: katsuyas@clin.medic.mie-u.ac.jp

Publication data
Submitted 22 August 2007
First decision 8 September 2007
Resubmitted 12 October 2007
Second decision 7 November 2007
Resubmitted 29 December 2007
Third decision 5 January 2008
Resubmitted 19 January 2008
Accepted 19 January 2008
Epub OnlineAccepted 22 January 2008

SUMMARY

Background

Radiofrequency ablation (RFA) therapy for hepatocellular carcinoma has enabled good local control to be possible. However, after successful local control, distant recurrences frequently occur in the remnant liver.

Aim

To identify the predictive factors for distant recurrence after RFA.

Methods

A total of 117 patients with initial non-advanced hepatocellular carcinoma with HCV who underwent RFA in our hospital were selected for this study. After transcatheter chemoembolization, RFA was performed under real-time computed tomography-fluoroscopic guidance. We studied survival rates, local (adjacent to treated tumour) and distant (intrahepatic site distant from the treated tumours) recurrence rates, as well as predictive factors for distant recurrence.

Results

After RFA, survival rates were 98.2% and 64.7% at 1 and 5 years, respectively. Child B patients had a significantly worse survival than Child A. Recurrence rates were 2.4% at 5 years for local, and 17.1% and 76.9% at 1 and 5 years, respectively, for distant. The Kaplan–Meier method revealed significantly high recurrence rates in cases with low albumin levels (Alb < 3.5 g/dL), high aspartate aminotransferase levels (AST > 60 IU/L), high alanine aminotransferase levels (ALT > 60 IU/L), low platelet counts (Plt < $10 \times 10^4/\mu$L), and high alpha-fetoprotein levels (AFP > 50 ng/mL). On multivariate analysis, low Alb levels and high AST levels were independent predictive factors for distant recurrence.

Conclusions

Although RFA enables good local control for initial hepatocellular carcinoma, distant recurrence is observed at high rates in HCV patients. Low albumin and high AST levels are predictive factors for distant recurrence.

Aliment Pharmacol Ther **27**, 1253–1260

doi: 10.1111/j.1365-2036.2008.03627.x

INTRODUCTION

Hepatocellular carcinoma (HCC) is a common complication of liver cirrhosis, and one of the main causes of death in liver cirrhosis. Surgical resection is an effective treatment for prevention of local recurrence, but indications are limited because of the underlying liver function. As a local treatment, percutaneous ethanol injection therapy (PEIT) has also been performed, but the clinical effects are unsatisfactory. Radiofrequency ablation (RFA) was first described by Rossi *et al.*,[1] and is a relatively new technique for local HCC therapy with many studies having demonstrated its clinical utility and safety.[2, 3] Comparative studies have shown that RFA is superior to PEIT in achieving complete tumour necrosis and local control with fewer treatment sessions.[4, 5] Since RFA was introduced, the local recurrence rate has decreased.[5] In addition, we have shown that a combination therapy with RFA and transcatheter chemoembolization is a safe and practical treatment method that achieves good therapeutic effects in both small and large HCC lesions.[6, 7] Blood flow promotes heat loss, and reducing or eliminating blood flow during the RF procedure is known to increase the ablation volume.[7] Because HCC is supplied almost entirely by the hepatic arteries, RFA is more effective after blocking hepatic arterial blood flow.[7]

However, distant recurrence rates remain high. To improve the prognosis of HCC patients, it is thus important to determine the factors that influence distant recurrence, and to control distant recurrence.

The number of HCV-related HCC has increased in recent years. In Japan, frequency of patients with HCV-related HCC was 72%, which was much higher than HBV-related HCC (17%).[8] In Italy, the rate of HCV-related HCC is almost the same level.[9] In the United States, the rate of HCV-related HCC is increasing.[10] In Asian countries, HBV-related HCC are still dominant; however, universal vaccination at birth for HBV has been shown to be highly effective in reducing carrier rates in children as well as the incidence of chronic liver disease including HCC.[11] HCV-related HCC is attracting attention all over the world; therefore, this study focuses on HCV patients.

The purpose of this study was to analyse the clinical effects of transcatheter chemoembolization and RFA combination therapy in HCC, and to determine the predictive factors for distant recurrence of HCV-related HCC.

METHODS

Patients

One hundred and seventeen patients with initial HCC, who underwent RFA after transcatheter chemoembolization for treatment of HCC between April 2000 and September 2006, were included in this study. The following criteria were adopted for our investigation: single nodule of 5 cm or smaller in diameter or up to three nodules each 3 cm or smaller, Child-Pugh A and B, and absence of extrahepatic metastasis. Patient background data are summarized in Table 1. Patients were diagnosed as having hypervascular HCC and were admitted to the Department of Gastroenterology, Mie University Hospital. Among the 117 patients, there were 80 men and 37 women, with a mean age of 67.4 years. All patients were anti-HCV antibody positive. With regard to Child-Pugh classification, 93 (79%) patients were class A and 24 (21%) were class B.

Diagnosis of HCC was primarily established based on radiological findings and elevated values of tumour markers. Biopsy was not performed if ultrasonography, computed tomography (CT), and CT during hepatic arteriography (CTHA) and arterial portograpy (CTAP) were all indicative of HCC, and if alpha-fetoprotein (AFP) or des-gamma-carboxyprothrombin (DCP) levels were elevated. A total of 161 nodules were found in this study; 80 patients had a single HCC nodule, 30 had two nodules and seven had three. The mean maximum tumour diameter was 24.2 mm, and the mean follow-up period was 29.1 months (3.9–72.8 months).

Chemoembolization

All patients underwent chemoembolization prior to RFA. After coeliac, superior mesenteric and hepatic

Table 1. Patient characteristics

Total patients	117
Male/female	80/37
Mean age (year)	67.4 (43–87)
Child-Pugh grade	
A	93 (79%)
B	24 (21%)
Mean maximum tumour size (mm)	24.2 (10–50)
Number of tumour nodule	
Uninodular	80 (68%)
Multinodular	37 (32%)
Mean follow-up period (month)	29.1 (3.9–72.8)

arteriography, a 3F micro-catheter (Micro Pheret; William Cook Europe, Bjaevevskov, Denmark) was advanced into the arteries supplying each tumour. The hepatic arteries were embolized with gelatin sponge particles (Spongel; Yamanouchi, Tokyo, Japan) after a mixture of 2–8 mL iodized oil (Lipiodol Ultra-Fluid; Mitsui, Tokyo, Japan) and 40 mg of epirubicin hydrochloride (Farmorubicin; Kyowa Hakko, Tokyo, Japan) was injected into the arteries.

Radiofrequency ablation

Because the gelatin sponge remains in the tumour for 2–3 weeks after chemoembolization,[12] RFA was generally performed within 2 weeks of chemoembolization.

Radiofrequency ablation was performed using a 17-gage straight electrode with a 2- or 3-cm exposed tip (Cool-tip single needle; Radionics, Burlington, MA, USA) connected to an RF generator (Cool-tip RF generator, Radionics). Patients received 0.1 mg of fentanyl citrate (Fentanest; Sankyo, Tokyo, Japan) intravenously before RFA for analgesia, and antibiotics (cefoperazone sodium and SBT, Sulperazon; Pfizer, Tokyo, Japan) were administered before and for 2–3 days after RFA.

After local anesthesia, the RF electrode was inserted into the tumour under real time CT-fluoroscopic guidance. Under CT-fluoroscopy, bubble formation in the tumour does not prevent additional electrode insertion into the tumour and accumulation of iodized-oil in the tumour ensures that the electrode is precisely inserted into the tumour. Plural electrodes could be placed in the tumour depending on the size and shape, and the RF generator was then activated at each tumour site. We finished an ablation session within an hour. When ablation was not enough, the second ablation session was performed next week after the initial ablation. The endpoint of RFA was the presence of a well-defined area of non-enhancing tissue comprising the treated tumour with a tumour-free margin of at least 5 mm in the arterial and portal phases on enhanced CT imaging.

Therapeutic effects and diagnosis of recurrence

Contrast-enhanced CT was performed to evaluate local therapeutic effects 1 week after RFA. Subsequently, contrast-enhanced CT was performed every 3 months. In this study, eight cases were administered anti-viral therapy with interferon after RFA and HCV disappeared in three patients. Ursodeoxycholic acid 600 mg/day, was administered for most patients. Local recurrence of HCC was defined as development of an enhanced area on CT adjacent to treated tumour. Distant recurrence was defined as the appearance of new tumours at an intrahepatic site distant from the treated tumours. When recurrence was suspected, angiography together with CTAP and CTHA was performed.

Predictive factors for cumulative distant recurrence of HCV-related HCC

Predictive factors for cumulative distant recurrence of HCV-related HCC were evaluated. Thirteen clinical and tumour factors investigated were: age, gender, tumour size, number of nodules, Child-Pugh grade, platelet counts (Plt), serum albumin (Alb), total bilirubin (T-Bil), aspartate aminotransferase (AST), alanine aminotransferase (ALT), AFP, DCP levels and prothrombin time (PT).

Statistical analysis

Unpaired Student's *t*-test was used to compare averages between groups, and the chi-square test and Fisher's exact probability test were used to compare independence. Survival and recurrence rates were computed using Kaplan–Meier estimates, and the Kaplan–Meier method and log-rank test were used to analyse predictive factors for distant recurrence of HCC. In addition to age, gender, tumour size, tumour number, and variables that achieved statistical significance ($P < 0.05$) in univariate analysis were subsequently assessed by multivariate analysis using a Cox proportional hazards model. A P-value of <0.05 was considered statistically significant. Analyses were performed using the StatView statistics package (SAS Institute, Cary, NC, USA).

RESULTS

Survival rate after initial RFA

The overall survival rates after initial RFA were 98.2% and 64.7% at 1 and 5 years, respectively (Figure 1a). In the Child-A patients, survival rates were 100% and 86.7% at 1 and 4 years, respectively, whereas in the Child-B patients, survival rates were

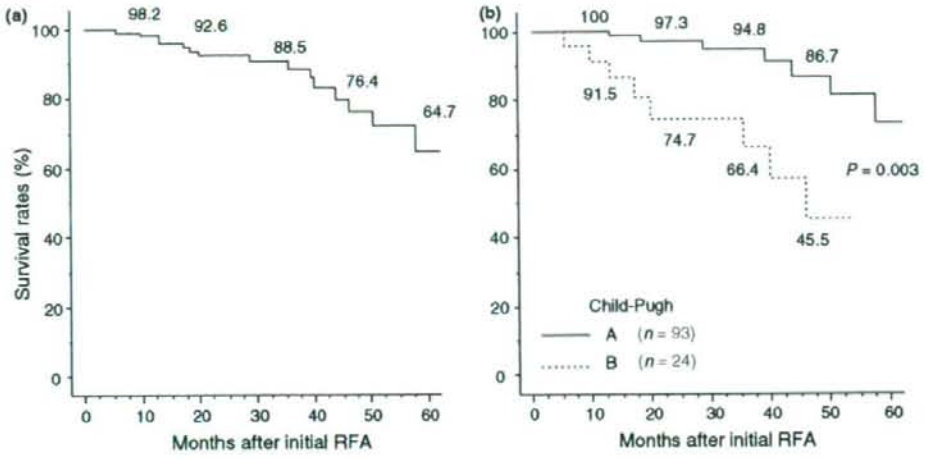

Figure 1. Overall survival rates after initial RFA and chemoembolization. Survival rates were 98.2%, 88.5% and 64.7% at 1, 3, and 5 years, respectively (a). In Child-A patients, survival rates were 100%, 94.8% and 86.7% at 1, 3, and 4 years, respectively (b). In Child-B patients, survival rates were 91.5%, 66.4% and 45.5% at 1, 3, and 4 years, respectively (b). RFA, radiofrequency ablation.

91.5% and 45.4% at 1 and 4 years, respectively (Figure 1b), with significant differences between the two groups.

Recurrence rate after initial RFA

Among 117 patients of this study, local recurrence was seen in two patients during the follow-up period. Locally recurrent tumours were treated by chemoembolization followed by RFA. The overall local recurrence rate was 2.4% at 5 years (Figure 2a). The overall distant recurrence rates were 17.1% and 76.9% at 1 and 5 years, respectively. (Figure 2b).

Background data of patients with recurrence of HCV-related HCC

Among the 117 patients of this study, distant recurrence of HCC in the remnant liver after complete coagulation was observed in 45 patients during the follow-up periods. Table 2 shows a comparison of baseline data before any therapy between patients with and without recurrence. No statistically significant differences were seen in age, gender, maximum tumour size, number of tumours, Child-Pugh grade, Plt, serum T-Bil, ALT, AFP, DCP and PT levels. Serum Alb level was significantly lower and AST level was significantly higher in the recurrence group ($P < 0.01$).

Therapy of patients with distant recurrence

On initial RFA, 79% of patients were Child A, though on recurrence, ratio of Child A was 65%. Six patients of Child A on initial RFA progressed to Child B on recurrence. Chemoembolization followed by RFA was performed again for 34 (79%) patients with distant recurrence, but eight were treated with palliative methods: four (9%) by transcatheter chemoembolization alone and four (9%) by continuous arterial infusion chemotherapy through a subcutaneously implanted port.

Predictive factors for cumulative distant recurrence

Table 3 shows the predictive factors for cumulative distant recurrence according to the Kaplan–Meier method in HCV patients. Significantly higher recurrence rates were seen in cases with low Alb levels, high AST levels, high ALT levels, high AFP levels and low Plt in monovariate analysis.

The predictive factors for cumulative distant recurrence after initial RFA according to Cox proportional hazard regression are low Alb levels and high AST

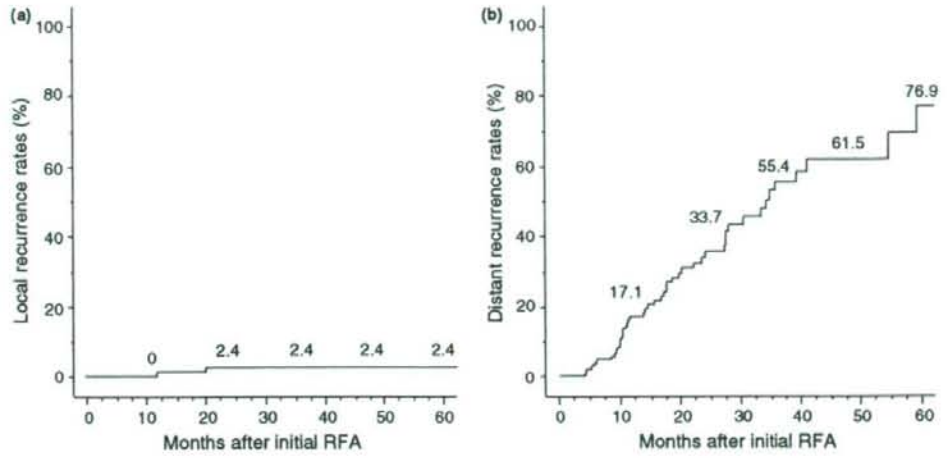

Figure 2. Local recurrence rates (a) and distant recurrence rates (b) after initial RFA and chemoembolization. Local recurrence rates were 2.4% at 5 years. Distant recurrence rates were 17.1%, 55.4% and 76.9% at 1, 3, and 5 years, respectively. RFA, radiofrequency ablation.

Table 2. Comparison of patients with and without distant recurrence

	Recurrence (n = 45)	No recurrence (n = 72)
Age (year)	66.5	67.9
Gender (male/female)	32/13	48/24
Maximum tumour size (mm)	24.5	24.0
Number of tumour nodule	1.49	1.30
Uninodular/multinodular	28/17	52/20
Child-Pugh (A/B)	34/11	59/13
Plt ($\times 10^4/\mu$L)	9.27	12.04
Alb (g/dL)	3.38	3.66**
T-Bil (mg/dL)	0.85	0.84
AST (IU/L)	82.6	64.5**
ALT (IU/L)	75.6	57.0
PT (%)	82.4	84.4
AFP (ng/mL)	175.5	105.6
DCP (mAU/mL)	203.5	171.5

Plt, platelet counts; Alb, albumin levels; T-Bil, total bilirubin; AST, aspartate aminotransferase levels; ALT, alanine aminotransferase levels; AFP, alpha-fetoprotein levels; PT, prothrombin time; DCP, des-gamma-carboxyprothrombin.
** $P < 0.01$.

Table 3. Predictive factors for distant recurrence (monovariate analysis)

Factors	P-value
Age (year) >70	0.63
Male	0.26
Tumour size >30 mm	0.85
Multinodular	0.10
Alb <3.5 g/dL	0.0050
T-Bil >1.0 mg/dL	0.61
AST >60 IU/L	<0.0001
ALT >60 IU/L	0.011
Plt $< 10 \times 10^4/\mu$L	0.0027
PT <80%	0.27
AFP >20 ng/mL	0.27
>50 ng/mL	0.034
DCP >40 mAU/mL	0.51
>100 mAU/ml	0.052

Plt, platelet counts; Alb, albumin levels; T-Bil, total bilirubin; AST, aspartate aminotransferase levels; ALT, alanine aminotransferase levels; AFP, alpha-fetoprotein levels; PT, prothrombin time; DCP, des-gamma-carboxyprothrombin.

levels (Table 4). In patients with high AST levels (>60 IU/L) and low Alb levels (<3.5 mg/dL), recurrence rates at 3 years were 74.8% and 79.2%, respectively (Figure 3).

DISCUSSION

In patients with HCV, especially with cirrhosis, HCC recurs even though local control is achieved. With regard to treatment of HCC, it is important to balance

Table 4. Predictive factors for distant recurrence (multivariate analysis)

Factors	Relative risk	95% C.I.	*P*-value
Male	1.617	0.670–3.900	0.2847
Age >70	1.354	0.603–3.038	0.4625
Tumour size >30 mm	0.753	0.311–1.825	0.5295
Multinodular	1.524	0.746–3.112	0.2479
Alb <3.5 g/dL	2.251	1.005–5.042	0.0485
AST >60 IU/L	4.318	1.918–9.721	0.0004
T-Bil >1.0 mg/dL	0.553	0.234–1.309	0.1778
Plt $<10 \times 10^4/\mu L$	2.001	0.943–4.249	0.0958
PT <70%	1.459	0.463–4.594	0.5185
AFP >50 ng/mL	1.751	0.880–3.479	0.0862

Plt, platelet counts; Alb, albumin levels; T-Bil, total bilirubin; AST, aspartate aminotransferase levels; AFP, alpha-fetoprotein levels; PT, prothrombin time.

tumour curability with preservation of liver function. The treatment method, which has good local control rates and small detrimental effects on liver function, should be selected for initial HCC. In recent years, RFA has been conducted as a local treatment for HCC, and has allowed fine local control.[5] Next problem to solve regarding HCC treatment, is how to control distant recurrence. Thus, determining the predictive factors for distant recurrence can assist in identifying, treating and possibly preventing HCC recurrence in HCV patients. In this study, we analysed the distant recurrence of HCC after RFA in patients of HCV-related HCC.

The 1- and 2-year local recurrence rates of HCC have been reported to be 1.3–18% and 2.4–37%, respectively, after RF alone,[3, 13–15] and 3.4–17% and 7.1–38%, respectively, after PEIT.[4, 5, 16, 17] In this study, local recurrence rates were 2.4% at 5 years. Recent studies reported insufficient ablative margin and large tumour (>30 mm) were the risk factors of local recurrence.[13] Considering 17% of patients in this study had HCC nodules larger than 30 mm, the local recurrence rates in this study were better than those reported previously. An ablated margin of 5 mm contributed to achieving local control. The combination of chemoembolization and RFA, and the use of real-time CT guidance also contributed to good local control. Decreased flow of blood enlarges the size of the necrotic area in RFA, and chemoembolization itself has an anticancer effect on HCC nodules.[7, 18] Real-time CT guidance is very useful for ensuring precise positioning of electrode insertion into the HCC nodules even if the lesion is located in the subcapsular or subphrenic region, and is thus useful for obtaining sufficient ablated margins.[7]

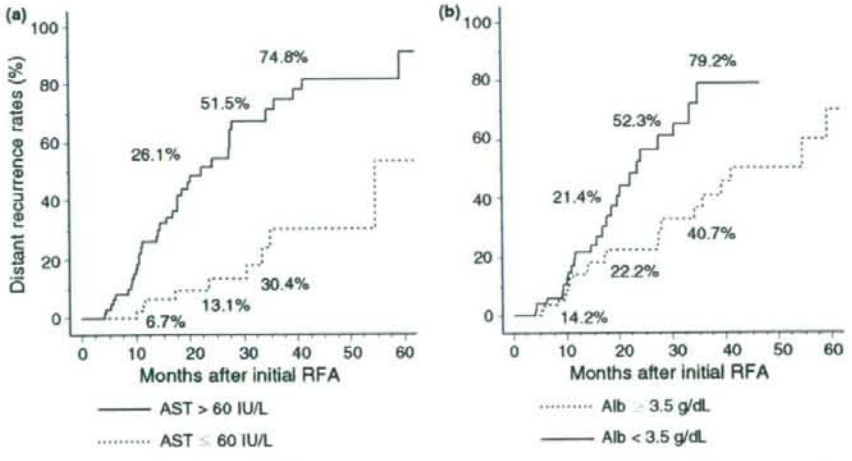

Figure 3. Cumulative distant recurrence rates based on (a) serum AST levels or (b) serum albumin levels. Three-year recurrence rates for patients with serum AST of >60 IU/L and ≤60 IU/L were 74.8% and 30.4%, respectively. Three-year recurrence rates for patients with serum albumin of ≥3.5 mg/dL and <3.5 mg/dL were 40.7% and 79.2%, respectively. AST, aspartate aminotransferase levels.

Despite good control of treated lesions, new tumours frequently occur in the untreated liver, resulting in high distant recurrence rates. Previous studies have reported distant recurrence rates of 18.7–22.5%, 62.1–67% and 81–81.7% at 1, 3 and 5 years, respectively, after PEIT,[16, 17, 19] 38% and 60% at 1 and 2 years, respectively, after RFA,[18] and 18% and 52% at 1 and 2 years, respectively, after RFA or microwave coagulation therapy.[20] In this study, distant recurrence occurred at 17.1%, 55.4% and 76.9% at 1, 3 and 5 years, respectively, which were comparable to those reported previously.

Factors affecting distant recurrence of HCC after PEIT reportedly include tumour size, nodule number, serum AFP level,[17] serum DCP level,[19] and indocyanine green retention rate at 15 min.[16] Meanwhile, risk factors for tumour recurrence after curative resection reportedly include not only tumour-related factors, such as nodule number and histological classification,[21] but also liver-related factors, such as serum ALT and serum Alb.[22, 23] After RFA, age[24] and nodule number[18] reportedly affected the distant recurrence. Another study reported that HCV infection and multinodularity were risk factors for distant recurrence.[20] However, few reports have suggested that stage of chronic liver disease affects recurrence.[21] In this study, low Alb (<3.5 mg/dL), high AST (>60 IU/L), high ALT (>60 IU/L), low Plt ($<10 \times 10^4$) and high AFP (>50 ng/mL) were predictive factors for distant recurrence on univariate analysis. However, multivariate analysis demonstrated that low Alb and high AST were independent predictive factors for cumulative distant recurrence. Thus, the state of the underlying liver has a greater influence on distant recurrence of HCC after RFA than tumour-related factors. Active inflammation in the non-tumorous area and impairment of liver function are associated with distant recurrence. We usually regard HCV patients with active hepatitis or cirrhosis as the high risk group for HCC occurrence and follow-up with close observation for biochemical studies, tumour markers and image studies. A high risk group of carcinogenesis has also higher possibility of recurrence of HCV-related HCC. Chemoembolization followed by RFA is apparently a good therapeutic modality to the point that tumour-related factors have little influence on distant recurrence.

In this study, overall survival rates after initial RFA were 98.2% and 64.7% at 1 and 5 years respectively, which are as good as or better than previous reports.[15, 25] In this study, after initial RFA, when recurrence occurred, 21% of distant recurrent tumours could not be treated by RFA, and such patients should be considered for liver transplantation.

In conclusion, chemoembolization followed by RFA is a good treatment for HCV-related HCC, but patients with abnormal AST levels and low Alb levels comprise a high-risk group for distant recurrence after RFA. Thus, tight follow-up with biochemical observation, tumour marker analysis and imaging studies are all essential for such patients. Furthermore, there is a pressing need to establish a strategy for preventing distant recurrence after RFA.

ACKNOWLEDGEMENT

Declaration of personal and funding interests: None.

REFERENCES

1 Rossi S, Di Stasi M, Buscarini E, *et al.* Cavanna L, Percutaneous radiofrequency interstitial thermal ablation in the treatment of small hepatocellular carcinoma. *Cancer J Sci Am* 1995; 1: 73–81.

2 Yamakado K, Nakatsuka A, Akeboshi M, Takeda K. Percutaneous radiofrequency ablation of liver neoplasms adjacent to the gastrointestinal tract after balloon catheter interposition. *J Vasc Interv Radiol* 2003; 14: 1184–6.

3 Yamakado K, Nakatsuka A, Akeboshi M, Takaki H, Takeda K. Percutaneous radiofrequency ablation for the treatment of liver neoplasms in the caudate lobe left of the vena cava: electrode placement through the left lobe of the liver under CT-fluoroscopic guidance. *Cardiovasc Intervent Radiol* 2005; 28: 638–40.

4 Ikeda M, Okada S, Ueno H, Okusaka T, Kuriyama H. Radiofrequency ablation and percutaneous ethanol injection in patients with small hepatocellular carcinoma: a comparative study. *Jpn J Clin Oncol* 2001; 31: 322–6.

5 Lencioni RA, Allgaier HP, Cioni D, *et al.* Small hepatocellular carcinoma in cirrhosis: randomized comparison of radio-frequency thermal ablation versus percutaneous ethanol injection. *Radiology* 2003; 228: 235–40.

6 Yamakado K, Nakatsuka A, Akeboshi M, Shiraki K, Nakano T, Takeda K. Combination therapy with radiofrequency ablation and transcatheter chemoembolization for the treatment of hepatocellular carcinoma: short-term recurrences and survival. *Oncol Rep* 2004; 11: 105–9.

7 Yamakado K, Nakatsuka A, Ohmori S, *et al.* Radiofrequency ablation combined with chemoembolization in hepatocellular carcinoma: treatment response based on tumor size and morphology. *J Vasc Interv Radiol* 2002; 13: 1225–32.